Final Draft
of the original manuscript:

Wang, L.; Oehring, M.; Liu, Y.; Lorenz, U.; Pyczak, F.:
Site occupancy of alloying elements in the L12 structure determined by channeling enhanced microanalysis in Gamma/Gamma' Co-9Al-9W-2X alloys.
In: Acta Materialia. Vol. 162 (2019) 176 - 188.
First published online by Elsevier: 26.09.2018

DOI: 10.1016/j.actamat.2018.09.059
https://dx.doi.org/10.1016/j.actamat.2018.09.059

Site occupancy of alloying elements in the $L1_2$ structure determined by channeling enhanced microanalysis in γ/γ' Co-9Al-9W-2X alloys

*Li Wang[1], Michael Oehring[1], Yong Liu[2], Uwe Lorenz[1], Florian Pyczak[1,3]

[1]Institute of Materials Research, Helmholtz-Zentrum Geesthacht, Max-Planck-Strasse 1, Geesthacht, D-21502, Germany

[2]State Key Laboratory of Powder Metallurgy, Central South University, Changsha, 410083, China

[3]Brandenburgische Technische Universität Cottbus-Senftenberg, Konrad-Wachsmann-Allee 17, Cottbus, D-03046, Germany

* Corresponding author: Tel.: +49 4152-87-2672; fax: +49 4152-87-2534

E-Mail: Li.wang1@hzg.de, wlyydy860601@hotmail.com (Li Wang)

Abstract

Knowledge about the sublattice site preference of alloying elements in the $L1_2$-γ' phase of novel Co-base superalloys is a necessary pre-requisite to understand their influence on the properties of the alloys in general and the γ' phase in particular. In the present study, the atomic site occupancy of the alloying elements in the $L1_2$-γ' structure in Co-9Al-9W-2X quaternary alloys after long-term annealing at 900 °C for 5000 hours was determined using the atom location by channeling enhanced microanalysis (ALCHEMI) technique in combination with energy-dispersive X-ray spectroscopy (EDX) composition analysis in a transmission electron microscope (TEM). The experimental ALCHEMI data were evaluated by comparing them with those calculated by the program 'Inelastic Cross Section Calculator' (*ICSC*). The results show that Co mainly occupies one sublattice site and Al/W are located at the other sublattice site in the $L1_2$ unit cell in the ternary alloy. The additional elements Ti, V, Mo and Ta which partition strongly to the γ' phase tend to occupy the Al/W sublattice site, and Cr which partitions more to the γ phase also favors the Al/W sublattice site, while Ni weakly partitions into the γ' phase and favors the Co sublattice site. The results of this study can provide evidence to the predictions on the site preference in literature based on the phase composition or on theoretical studies.

Keywords

Cobalt-base superalloys; ALCHEMI; Site occupancy; $L1_2$ compound; EDX in TEM;

1. Introduction

The reports about an ordered $L1_2$ precipitate ($Co_3(Al, W)$) phase in the ternary Co-Al-W system in 2006 which can be stable up to temperatures of 950 °C have attracted significant research interest [1]. The low mismatch between the fcc γ-Co solid solution phase and the $L1_2$ γ'-Co_3 (Al, W) phase helps to establish a microstructure with a high volume fraction of coherent cuboidal γ' precipitates embedded in a continuous γ matrix [2]. This opens for Co-base alloys the perspective to benefit from the same precipitation hardening mechanism that works so efficiently in Ni-base superalloys. However, recently the γ' phase has been reported to be metastable in the ternary Co-Al-W system [3]. In order to increase the temperature capability and stabilize the $L1_2$-γ' phase, additional elements such as Ni, Ti, Ta, Nb, Mo and V are alloyed to the ternary Co-Al-W system [4-6]. It is found that Mo, V, Nb, Ta and Ti partition to the γ' phase and thus increase the γ' solvus temperature of Co-Al-W superalloys, while, Fe, Mn and Cr partition to the γ phase and decrease the amount of the γ' phase [1, 7, 8]. With increasing Ni content in the Co-Ni-Al-W system, the γ' solvus temperature increases and the γ+γ' two-phase region is broadened [9]. The partitioning and site preferences of additional elements effects the γ' solvus temperature and lattice mismatch between the γ and γ' phases and can strongly influence the electronic bonding, antiphase boundary and stacking fault energy as well as the resistance to dislocation motion [4]. It is important to investigate these basic structural properties to understand the effects of different alloying elements on a wide variety of alloy properties. Thus, knowledge about the partitioning behavior and site occupancy of alloying elements is a valuable prerequisite to further optimize and develop these novel γ/γ' Co-base superalloys.

The atomic site preference of several alloying elements in the γ' phase of Co-base superalloys has been predicted theoretically utilizing first principles and thermodynamic calculations [4, 10-12]. However, direct experimental investigations are relatively rarely found in the literature. Some researchers tried to use atom probe tomography (APT) to determine the lattice site occupancy of the alloying elements, but the individual atomic layers in the atom maps could not be resolved due to the limited spatial resolution in pulsed laser mode [13, 14]. In other APT work in the voltage operation mode it could be shown that Al, W and Mo or Ta occupied the same atomic planes, but the pure Co planes were still not resolved in the APT

reconstruction [15]. Recently, in a Co-12Ti system investigated by APT in the pulsed laser mode, the additions of Mo and Cr were reported to preferentially occupy the Ti sublattice site based on the element-specific spatial distribution maps along the [001] direction of the γ' phase [16]. Using a combination of aberration corrected high-angle annular dark field (HAADF) scanning transmission electron microscopy (STEM) and energy dispersive X-ray spectroscopy (EDX) with a four-quadrant FEI Super-X detector the site preferences of Co, Al, W, Ti and Ta in the $L1_2$-γ' unit cell in Co-base superalloys have been investigated experimentally [17]. However, it should be mentioned that the alloys investigated in these studies were only annealed for a short time. Thus, the measured phase compositions and atomic site occupancies might deviate from those under equilibrium conditions.

The method of atom location by channeling-enhanced microanalysis (ALCHEMI) which was first developed by Taftø and Spence [18, 19], has been widely used to determine the crystallographic sites, distribution and chemical nature of substitutional impurities in alloys, such as TiAl alloys [20], Ni-base alloys [21], B2-(Ni, Fe)Al phase [22] and Nb-Cr-X Laves phase [23]. It is a transmission electron microscopy (TEM) technique based on the orientation-dependence of characteristic X-ray emissions of alloying elements [24]. Because the initial formulations of ratio ALCHEMI did not consider the effect of delocalization of the inner-shell ionization event and anti-site defects, significant errors and unphysical site occupancies can result [25-27]. To solve these problems, approaches such as using correction factors [26, 28], statistical analysis of the data acquired from a variety of orientations [29, 30] or incorporating the anti-site defect concentration into the formulation [31] have been developed. Recently, the characteristic X-ray intensities were measured at various electron incidence directions and by comparison with the X-ray intensities calculated from first principles, or with the inelastic scattering cross-sections calculated by the *ICSC* program developed by Oxley and Allen [32] it was possible to determine the atomic site occupancies in thermoelectric materials [33] and the dopant cation site in oxygen separation membrane materials [34].

In this study, the atomic location of alloying elements in the $L1_2$-γ' unit cell in Co-9Al-9W-2X (X= Ti, V, Cr, Ni, Mo and Ta) alloys after long-term annealing was investigated by planar ALCHEMI. To the authors' knowledge, this is the first work which applies ALCHEMI to γ-γ' Co-base superalloys and also the first experimental investigation of the site preferences of a wide selection of elements in the γ' phase.

Additionally, the experimental results have been compared with calculated inelastic ionization scattering cross-sections using the *ICSC* program [32]. Finally, by quantifying the experimental ALCHEMI data with aid of the measured chemical composition of the γ' phase after annealing at 900 °C for 5000 h, the site occupancy of the alloying elements in the $L1_2$-γ' unit cell has been confirmed. It is believed that this work can be instructive for both theoretical and experimental studies on the alloy design for the new type of γ-γ' Co-base superalloys.

2. Inelastic scattering cross-section calculation by *ICSC*

The program *ICSC* (Inelastic Cross Section Calculator) developed by Oxley and Allen [32] was applied to calculate the inelastic scattering cross-sections of alloying elements, which were compared with the experimental characteristic X-ray intensities. Based on the formulas in refs. [32, 35], the ionization cross-section σ contains contributions from dynamically scattered electrons and also "dechannelled" electrons (mainly thermal diffuse scattering). In the current calculations, the unit cell of the $L1_2$ γ'-Co_3(Al, W) phase is defined as a cube with Co atoms occupying the face-centered sites, while Al and W occupy the corner sites equally. In order to simplify the calculation, the additional element Ti, V, Cr, Ni, Mo or Ta was treated as an impurity in the $L1_2$ phase because its contribution to the thermal diffuse scattering is not significant. When calculating the inelastic scattering cross-sections, with or without including the root-mean-square thermal atomic displacements of the quaternary elements, no significant differences were noticed in the simulated inelastic scattering cross-sections. Thus, only the root-mean-square thermal atomic displacements of Co, Al and W atoms which at about room temperature are 0.0060 [25], 0.0095 and 0.0019 $Å^2$ [36], respectively were imported into the program for calculating the thermal diffuse scattering coefficients. Because the ionization scattering factors for X-ray emission in the program were only parameterized for $6 \leq Z \leq 50$ for K-shell ionization and $20 \leq Z \leq 60$ for L-shell ionization, the cross-sections for W and Ta could not be calculated.

Experimental parameters such as electron voltage, specimen thickness and convergence angle influence the inelastic scattering cross-sections of the alloying elements, and thus affect the enhancement or attenuation of the emission of characteristic X-rays. **Fig. 1** shows the calculated normalized inelastic scattering cross-sections of the base element lines Co-K and Al-K. The cross-sections were plotted as a

function of scattering conditions along the 002 Kikuchi band with a maximum Bragg angle of 20.9 mrad for ±006 reflections in the <001> zone axis of the $L1_2$ γ'-Co_3(Al, W) phase. In order to make the channeling effects of the alloying elements easily visible in the $L1_2$ phase, the cross-sections were firstly normalized by the cross-sections under kinematical condition and then normalized by the cross-section of the Co-K line, namely (σ_d/σ_k)-X/(σ_d/σ_k)-Co_K (X is alloying element). Thus, the normalized Co-K cross-section remains unity while the normalized cross-section of other elements, such as Al can show the channeling effects when the scattering condition changes. When changing the (a) convergence angle, (b) voltage, and (c) specimen thickness, the channeling intensity varies. If the convergence angle is increased from 2 to 4 mrad (voltage kept at 200 kV and specimen thickness at 100 nm), the channeling effect of the normalized Al-K cross-section is less pronounced. As increasing the convergence angle, the ionization cross-sections slightly decrease and the channeling intensity of the normalized Al-K cross-section is also slightly reduced. This stems from the fact that the channeling condition is fulfilled for a planar incident electron wave and thus a bigger convergence angle causes a higher deviation of the incident beam from such an ideal planar wave character, resulting in a reduced channeling intensity [37, 38]. On increasing the electron voltage (convergence angle kept at 4 mrad and specimen thickness at 100 nm), the normalized cross-section profiles of the Al-K line change obviously, especially for scattering conditions between the (00-2) and the (002) reflections. Increasing the electron voltage, the peak at $k_x/g_{001} = 0$ gradually becomes lower and broader and disappears finally. From the calculations it is found that the effects from delocalization on the cross-section increase with acceleration voltage and are stronger for the characteristic X-ray emission with lower energy [24, 26, 35]. A lower voltage can reduce the delocalization effects and show better channeling effects. But for better statistic it is recommended to use a higher voltage to get more X-ray counts and improve the peak/background ratio. Thus choosing an acceleration voltage of 200 kV could balance the effects from delocalization and X-ray counts. Also the normalized cross-section of Al-K still shows similar channeling features at 200 kV as at 80 kV voltage. Varying specimen thickness can also influence the normalized cross-section profiles and the channeling intensity is less pronounced with increasing foil thickness (convergence angle kept at 4 mrad and voltage at 200 kV). The calculated cross-sections show that the contribution from the dynamical scattering decreases while the kinematical component of the ionization cross-sections increases with thickness

resulting in a decrease in the ionization cross-sections. Thus, the channeling intensity reduces with increasing thickness [26, 32-34]. Between the (00-2) and the (002) reflections, there is no peak in the normalized cross-section profile for a specimen thickness of 20 nm. Increasing the thickness to 60 nm results in the appearance of an obvious peak but it becomes broader and finally disappears when the thickness is further increased to 200 nm.

3. Experimental

3.1 Specimen preparation

Alloys with nominal compositions of Co-9Al-9W and Co-9Al-9W-2X (Ti, V, Cr, Ni, Mo and Ta) (atomic percent are used throughout the paper, at.%) were produced by arc-melting and re-melted at least eight times to obtain chemical homogeneity. The cast specimens were then homogenized at 1300 °C for 12 h and annealed at 900 °C for 5000 h. TEM foils with a diameter of 2.3 mm were ground to a thickness below 120 μm and then thinned by twin-jet polishing at 25-35 V and a temperature of -40 °C with a solution of 26 ml perchloric acid (70%), 359 ml 2-butanol and 625 ml methanol.

3.2 Planar ALCHEMI investigations

The ALCHEMI investigations were conducted in the three orientations <001>, <110> and <111> of the γ' phase, as shown in **Fig. 2**a. These directions are well suited because when looking along these orientations the atomic planes are composed of alternate Co planes and mixed planes of Co, Al and W. The TEM specimens were first tilted away from the zone axis <001>, <110> or <111> along the Kikuchi band 002, 2-20 or 02-2, respectively, by around 5° to get systematic row reflections. X-ray spectra were then acquired by an energy-dispersive detector under different diffraction conditions vertical to the chosen Kikuchi band by tilting the beam incidence direction using the electron beam tilt controls instead of tilting the specimen. Additionally, spectra were collected under the kinematical (non-channelling) scattering condition via tilting the specimens. All the spectra were collected using the longest process time available with the analysis system to get the best X-ray peak resolution. All investigations were done using a Philips CM200 transmission electron microscope (TEM) operated at 200 kV equipped with an Oxford instrument X-mas EDX analysis system. Characteristic X-ray intensities of the alloying elements were obtained by integrating the Co-K, Al-K, W-L, W-M, Ti-K, V-K, Cr-K, Ni-K, Ni-L, Mo-K, Mo-L, Ta-L, or Ta-M

peaks in the spectra which were directly read out from the Oxford Inca software. Using the software the background was subtracted and integrated intensities were determined by fitting peak profiles to the measured intensities. **Fig. 2**b shows an example of a one-dimensional scan over the reciprocal space between the (-440) and the (4-40) reflection (Bragg angle 19.7 mrad) near the <111> orientation. For each EDX spectrum the collecting time was varied to get a similar number of counts (20000) for the Co-$K_{\alpha 1}$ peak in every spectrum. In order to get more intensity, a large condenser aperture (condenser aperture 4 / 200 µm) was used resulting in a convergence angle of 4 mrad which was determined by analysing the diffraction pattern. The experiments were conducted at room temperature.

Based on the calculated results in **Section 2** and the experimental conditions, a voltage of 200 kV and a convergence angle of 4 mrad (condenser aperture 4 / 200 µm) were used for ALCHEMI investigations. As mentioned before an acceleration voltage of 200 kV was chosen to balance the effects from delocalization and X-ray counts. If a smaller convergence angle, for example, 2 mrad (condenser aperture 3 / 75 µm) was used, the channeling intensity would be improved. However, the X-ray signal would have a lower intensity and a longer spectrum collection time would have been required. This could have caused difficulties in interpreting the results due to specimen drift, worse signal to background ratio and contamination. Taking **Fig. 3** as an example, an AlCHEMI study was carried out in the marked γ' region. Obvious contamination can be observed after the investigation even with the large condenser aperture 4. This could change the specimen thickness locally, and thus influence the X-ray intensities due to absorption. The local thicknesses of the regions used for the ALCHEMI study were estimated to be in the range of 100 to 200 nm using the convergent-beam electron diffraction technique. For this specimen thickness good channeling effects and clear Kikuchi bands were obtained.

3.3 EDX phase composition analysis

Elemental analysis of the γ' phase for each alloy composition was done using EDX in the TEM mode. The composition was averaged from at least ten γ' precipitates in different regions with a similar foil thickness and tilt condition. To avoid channelling effects the specimen was tilted away from a symmetric diffraction condition so that no reflections were strongly activated. Concentrations of the elements Co, Al and W were quantified with a Co-2Al-2W alloy standard.

4. Results

4.1 Atomic site occupancy of alloying elements in the $L1_2$-γ' structure by ALCHEMI

Fig. 4 shows examples of EDX spectra acquired at *s*<0, *s*>0 with respect to the 011 reflection and kinematical scattering conditions near the <100> direction in the (a) Co-9Al-9W-2Ti and (b) Co-9Al-9W-2Ni alloys, respectively. In the enlarged image profiles, it is obvious that in both alloys the emissions of Al-K, W-L and W-M X-rays are enhanced at *s*<0 and depressed at *s*>0 compared to those under kinematical scattering conditions. This indicates that the ionization events are intensified on the Al and W containing lattice planes at *s*<0, relative to the Co containing lattice planes at *s*>0. This is different to the situation in the Ni_3Al phase where at *s*>0 the emission of Al-K is increased while at *s*<0 the emission of Ni-K is enhanced [21]. The projected absorptive potential in the <100> zone axis of the Co_3(Al, W) phase (lattice parameter 3.60 Å) was calculated using the multi-slice method in the JEMS software (Version 4.6228U2018, Stadelmann P.). It is found that the sublattice site with Al/W atoms (28.1 V) has a higher absorptive potential than the Co sublattice site (9.3 V), which is caused by the larger atomic number of W atoms compared to Co atoms. When the scattering condition changes the emission of Ti-K X-rays in the Co-9Al-9W-2Ti alloy shows a similar variation to those of the Al-K, W-L and W-M X-rays, while the emission of Ni-K X-rays in the Co-9Al-9W-2Ni alloy remains nearly constant, similar to that of Co-K X-rays. From these results, it can be inferred that Ti atoms favor the Al/W sites but Ni atoms preferably occupy the Co sites in the $L1_2$ structure.

In **Fig. 5** to **Fig. 9**, the normalized integrated intensities of alloying elements were plotted as a function of scattering vectors from the (-004) to the (004) reflection or from the (0-4-4) to the (044) reflection near the <001> and the <011> zone axes, and from the (-440) to the (4-40) reflection near the <111> zone axis. The X-ray intensities were first normalized by the intensities obtained under kinematical conditions and then normalized by the intensities of the Co-K lines. Thus, the normalized Co-K intensity profile has a value of unity when changing the scattering vector. Additionally, in order to compare with the experimental ALCHEMI results and to further confirm the atomic location of alloying elements, normalized inelastic scattering cross-sections of the investigated elements have been calculated using the *ICSC* program [32], as shown in **Fig. 10**. This has been done for all elements except W and Ta because the

ionization scattering factors of the respective X-ray energies are not covered within the *ICSC* program. All the cross-sections were first normalized by those under kinematical condition and then by the cross-section of the Co-K X-ray emission. The voltage, specimen thickness and convergence angle used for these calculations are 200 kV, 100 nm and 4 mrad, respectively. It is found that when the scattering vectors are perpendicular to the same Kikuchi band, the cross-sections remain the same along different orientations. Thus, the calculated inelastic cross-sections are plotted against the scattering vectors which are perpendicular to the Kikuchi bands (002) and (02-2) near the <001> direction. **Fig. 10**a, c shows the situation when the alloying elements occupy the Al-site and **Fig. 10**b**,** d when they are located on the Co-site. By measuring the characteristic X-ray intensities at various diffraction conditions and comparing the results with the calculated data, a better accuracy about the atomic site occupancy of the alloying elements can be obtained because these intensity profiles strongly indicate the atom locations on different sublattices in the $L1_2$ unit cell.

Fig. 5 shows the normalized intensity profiles of Co-K, Al-K, W-L and W-M as a function of scattering vectors perpendicular to the (002) Kikuchi band in the <011> zone axis and the (2-20) Kikuchi band in the <111> zone axis for the ternary Co-9Al-9W alloys. In **Fig. 5**a the normalized intensity profiles of Al-K and W-M reveal a very similar behavior. The emissions of the Al-K and W-M X-rays are enhanced near to the ±(400) reflections and reduced at $k_x/g_{100} = 0$. The behavior of the intensity profile of the W-L peak is different, with the emission of the W-L X-rays increased at $k_x/g_{100} = 0$ after a decline around $k_x/g_{100} = \pm 2$. This could probably be attributed to different delocalization and absorption parameters for the emission of characteristic X-rays for the L-line [25, 39]. In this case we think that the effects from the X-ray absorption are less important than those from delocalization. This was supported by performing an absorption correction for the characteristic X-rays which had no obvious influence on the normalized intensity profiles plotted against scattering vectors. When collecting EDX spectra, since the tilt angle and the specimen thickness were the same for all dynamical scattering conditions and did not vary so much from those under the kinematical scattering conditions, the normalized intensity should be not greatly affected by absorption as it should be similar for all X-ray intensities. This difference is less pronounced for the normalized intensity profiles as a function of scattering vector perpendicular to the (2-20) Kikuchi band as shown in **Fig. 5**b. The emissions of Al-K, W-L as well as W-M X-ray radiation are all enhanced near the

systematical row reflection condition ($k_x/g_{1\text{-}10}$ = 0) but depressed close to the ±(2-20) reflections. These results show that Al and W atoms occupy the same sublattice site and Co atoms are located on the other sublattice site. Thus the elements occupy the atomic sites which could already be assumed based on the stoichiometry of the Co_3(Al, W) γ' phase [1, 13-15].

Figs. 6-8 show the ALCHEMI results for the quaternary Co-9Al-9W-2Ti, Co-9Al-9W-2V, Co-9Al-9W-2Cr, Co-9Al-9W-2Mo and Co-9Al-9W-2Ta alloys. It is found that the intensity of the Ti-K, V-K, Cr-K, Mo-K, Mo-L, Ta-L and Ta-M X-ray emissions vary in a very similar way to those of the Al-K, W-L and W-M X-rays when changing the scattering conditions. Especially for the case when the intensity profiles were plotted as a function of the scattering vector from the (0-4-4) to the (044) reflection perpendicular to the (022) Kikuchi band (**Fig. 6**b, **7**b and **8**b), the emissions of the alloying elements are enhanced at k_x/g_{011} = 0 or ±4 and decreased at around k_x/g_{011} = ±2. With the scattering condition changing from the (00-4) to the (004) reflection vertical to the (002) Kikuchi band, the intensity variation of the Al-K X-ray emission behaves similarly to that of W-M in all the alloys. Similar behavior is seen for Ta-M in the Co-9Al-9W-2Ta alloy. However, the Ti-K, V-K, Cr-K and Ta-L intensity profiles vary similarly to that of W-L and the intensity is enhanced near to the ±(004) reflections and at k_x/g_{001} = 0, and decreased near the ±(002) reflections (**Fig. 6**a, **7**a and **8**a, c). The Al-K X-ray emission shows a slight enhancement at k_x/g_{001} = 0 in the Co-9Al-9W-2V (**Fig. 7**a), Co-9Al-9W-2Cr (**Fig. 8**a) and Co-9Al-9W-2Ta (**Fig. 8**c) alloys but not in the Co-9Al-9W-2Ti alloy (**Fig. 6**a). It is noteworthy that for the calculated inelastic cross sections, as shown in **Fig. 1**c, the enhancement of the Al-K cross-section near k_x/g_{001} = 0 is very sensitive to variations in specimen thickness and becomes less pronounced with increasing specimen thickness. Thus, the slight difference at k_x/g_{001} = 0 of the Al-K profiles in different alloys could be attributed to small thickness variations between the regions investigated. However, it could also be that the experimental data suffers from some scatter, and the increase in the intensity at k_x/g_{001} = 0 may sometimes be not clearly observed. In summary, the above experimental results imply that Ti, V, Cr, Mo and Ta preferentially occupy the same sublattice site as the Al and W atoms in the $L1_2$ structure.

In the Co-9Al-9W-2Ni alloy, as shown in **Fig. 9,** the Al-K and W-M X-ray emissions again vary similarly to that of W-L. However, the intensity profile of the Ni-K X-ray behaves similarly to that of Co-K, with its value only slightly fluctuating around one. Whereas, the emission of the Ni-L X-ray is enhanced near

k_x/g_{001} / k_x/g_{011} = ±4 but depressed at k_x/g_{001} / k_x/g_{011} = 0 when the scattering vector changes from the (00-4) to the (004) reflection vertical to the (002) Kikuchi band (**Fig. 9**a) and from the (0-4-4) to the (044) reflection perpendicular to the (022) Kikuchi band (**Fig. 9**b). The different behavior of the Ni-K and Ni-L X-rays which are both emitted by the same element, is also mirrored in the different behavior of these two X-ray emission intensities as predicted by the inelastic cross section calculations in **Fig. 10**b and d when Ni is assumed to occupy the Co-site in the lattice. Based on the above results it is proposed that Ni atoms prefer the Co-site in the $L1_2$ structure.

Fig. 10 shows the calculated normalized cross-section of the alloying elements plotted against the scattering vectors. When all the alloying elements were assumed to be located on the Al-site (**Fig. 10**a, c), their normalized cross-sections behave similarly to that of Al-K and show significant enhancement when varying the scattering vector. However, when assuming them to occupy the Co-site, the normalized cross-sections of alloying elements behave similarly to that of Co-K except for Mo-L and Ni-L which show obvious enhancements. Thus, by comparing the experimental ALCHEMI results with the calculated data, it is further confirmed that Ti, V, Cr, Mo or Ta atoms favor the Al/W site while Ni tends to occupy the Co site. It is interesting to note that the cross-sections of the alloying elements increase near the ±(004) reflections in **Fig. 10**a in the order of Ni-L > Al-K > Mo-L > Ti-K > V-K > Cr-K > Ni-K > Mo-K. This is the same order when the energies of the X-ray lines are arranged from lowest to highest. However, the cross-sections increase at k_x/g_{001} = 0 in a reversed order Ni-L < Al-K < Mo-L < Ti-K < V-K < Cr-K < Ni-K < Mo-K. This phenomenon is very similar to the profiles shown in **Fig. 10**c in which the enhancement of the cross-sections has the order of Ni-L > Al-K > Mo-L > Ti-K > V-K > Cr-K > Ni-K > Mo-K near $k_x/g_{01\text{-}1}$ = ±4 but again a reversed order of Ni-L < Al-K < Mo-L < Ti-K < V-K < Cr-K < Ni-K < Mo-K at $k_x/g_{01\text{-}1}$ = 0. The difference in the values of the normalized cross-sections for different characteristic X-ray energies could be due to the delocalization effects.

4.2 EDX analysis of the γ' phase

The chemical composition of the γ' phase in the Co-9Al-9W-2X alloys was examined by TEM-EDX and the results are shown in **Table 1.** The γ' phase composition of the Co-9Al-9W-2Ti/Mo/Ta alloys has already been published in [40] and is included here again to aid in understanding the results and

conclusions below. It is found that the γ' phase has a similar Co fraction in all the alloys of around 78-79 at.%, except for the Co-9Al-9W-2Ni alloy which has a slightly lower Co content of around 77 at.%. In the Co-9Al-9W base alloy, the γ' phase has a composition of (78.8±0.4) at.% Co, (9.2±0.2) at.% Al, and (12.1±0.3) at.% W. When considering the stoichiometry of the $L1_2$-Co_3(Al, W) phase, the fractions of elements should be 75, 12.5 and 12.5 at.% for Co, Al and W, respectively. Here, it is found that in the γ' phase, the content of Al is lower than that of W and that around 4 at.% of the Co atoms have to occupy the Al/W atomic sites. This excess of Co and deficit of Al in the γ' phase agrees with other studies in literature [1, 41] and also with calculations by density functional theory which found that placing Co on Al sites to form Co_{Al} anti-site defects is energetically favorable at 0 K [42]. In this study, in order to reduce the effects from X-ray absorption, the k-factors for Co, Al and W were determined using a standard. But it should be noted that the chemical composition measured for the γ' phase might be affected if there is residual γ matrix above or below the γ' phase. In the study by Povstugar et al. [13] the slight excess of the Co concentration above 75 at.% was thought to result from field evaporation artifacts of the atom probe tomography measurements instead of a non-stoichiometric γ' phase. Based on the γ' phase compositions from **Table 1**, the additional quaternary elements can be classified into three groups: a) Mo, V, Ti and Ta partition preferentially to the γ' phase with partitioning coefficients $K_{\gamma'/\gamma}$ of 1.2, 1.3, 2.2 and 6.3, respectively. When alloying with these elements, the fractions of Co and Al in the γ' phase do not show an obvious change or only slightly decrease, but the W content is reduced clearly; b) Cr strongly partitions into the γ matrix with a partitioning coefficient $K_{\gamma'/\gamma}$ = 0.6. The addition of Cr causes a slight decrease in the content of Co, Al and W in the γ' phase compared with their concentration in the ternary system; c) Ni shows a slight preferential partitioning to the γ' phase with $K_{\gamma'/\gamma}$ = 1.1. Its addition has almost no effect on the fraction of Al and W but results in an obvious decrease of the Co content in the γ' phase.

Here it should be noted that the small changes in the fraction of Al and W in the γ' phase of different alloys could also be due to other factors. The overall compositions of the bulk materials were measured to be 84Co-7Al-9W (at.%) for the ternary alloy and 82Co-7Al-9W-2X (at.%) for quaternary alloys. From weight-loss calculations of the starting elements and final ingots it is apparent that the Al fraction determined using SEM-EDX was underestimated for all alloys. Thus, the influence from the bulk alloy compositions on the variation of Al and W fractions could be ignored. However, scatter of the

measurements or the variation of the local specimen thickness could also introduce such small changes on the Al and W fractions.

5. Discussion

5.1 Comparison between experimental ALCHEMI results and calculations

The measured intensity profiles obtained by the experimental ALCHEMI studies agree very well with the normalized ionization cross-sections of the alloying elements calculated by the *ICSC* program. Although some differences can be seen, such as in the symmetry of the intensity profiles and the detailed normalized intensity value, the discrepancies might be due to the following reasons. The chemical composition of the γ' phase (Co 75.0%, Al 12.5% and W 12.5%) used in the calculation is different from the measured composition (**Table 1**), and the alloying elements are treated as impurities, which can influence the thermal diffuse scattering coefficients and thus the channeling intensity. Additionally, the thickness of the investigated regions might have differed from the thickness of 100 nm used in the calculations, which can affect the kinematical and dynamical component of the ionization cross-sections. Meanwhile, due to the long EDX spectra collecting time, contamination of the investigated regions increases the local foil thickness and thus changes the exact symmetry of the intensity profiles. It should be noted that effects from X-ray absorption in the depth of the specimen could be excluded due to the similar X-ray absorption factors under kinematical and channeling conditions [34].

5.2 Insights in the site occupancy judging from the γ' phase composition

From the TEM-EDX analysis in the present study, the additional alloying elements can be divided into three groups. In case of the elements Ti, V, Mo and Ta that strongly partition into the γ' phase but where the Co fraction of the γ' phase remains almost unchanged, it is indicated that these elements fully occupy the Al/W site in the γ' phase. Cr preferentially partitions to the γ phase, not only reducing the Co fraction, but also the fraction of Al and W in the γ' phase. Taking into account that the Co content in the γ' phase is slightly higher than the value expected based on the stoichiometry of the $L1_2$ structure, this could indicate that all Cr atoms occupy the same atomic site as Al/W and that some Co atoms occupying the Al/W site are redistributed to the γ phase. Another possibility is that Cr partially occupies the Al/W site and the remaining Cr atoms go to the Co site in the $L1_2$ structure. Ni has a weak partitioning tendency to the γ'

phase but clearly rejects some of the Co atoms from the γ' phase into the solid solution γ phase by occupying either the Al/W or Co sites.

5.3 Quantitative ALCHEMI analysis to determine site occupancy

It is not as easy to calculate the exact site occupancy of alloying elements in the $L1_2$-γ' phase by quantitative ALCHEMI as it is for other phases, such as Ni_3Al and TiAl, due to the Al/W atoms being both on one sublattice site and the large energy difference in the characteristic X-ray radiation of the alloying elements. Nevertheless, in the following we have tried to quantitatively calculate the site occupancy of additional elements using the formula:

$$\emptyset_{i/a} = \emptyset_{j/a} + (q_a - \emptyset_{j/a}) \frac{R_i - R_j}{\sum_k x_k (R_k - R_j)}, \quad (1)$$

developed by Horita et al. [43]. Where, $ø_{i/a}$ or $ø_{j/a}$ is the fraction of element *i* or *j* occupying the *a* site, q_a is the total fraction of *a* site in the unit cell, x_k is the atomic fraction of the alloying element and the ratio *R* is defined as

$$R = \frac{N^d}{N^k}, \quad (2)$$

where, N^d and N^k are the characteristic X-ray intensity under dynamical (channeling) and kinematical (non-channeling) conditions. Using the intensity ratios has the advantage that the absorption effects of the X-ray energy can be ignored because the absorption factors under dynamical and kinematical conditions are similar. From the EDX analysis of the γ' phase composition, it is known that the fraction of Co exceeds the stoichiometric value and some Co must be placed on Al/W sites to form $Co_{Al/W}$ anti-site defects. When one host element occupies antisite locations, formula (1) can be simplified to

$$\emptyset_{i/a} = 1 + (q_a - 1) \frac{R_i - R_A}{\sum_k x_k (R_k - R_A)}, \quad (3)$$

due to $ø_{A/a}$=1, where A is the hypo-stoichiometric element, in this case Al or W, q_a is 0.25 and x_k is known from the EDX analysis in **Table 1**. The value of R_i for different characteristic X-ray lines can be obtained from the EDX spectra under different scattering conditions.

Because the characteristic X-ray energy of the alloying elements ranges from Ni-$Lα_1$ (0.85 keV) to Mo-$Kα_1$ (17.48 keV), the delocalization of the characteristic X-ray emission of each element is different and

increases with decreasing X-ray energy. Pennycook [26] used the root-mean square impact parameters b_{rms} to characterize the degree of delocalization of the electron impact ionization interaction. A more accurate calculation for b_{rms} was proposed by Oxley and Allen [44] and the values for the characteristic X-rays of alloying elements at 200 keV electron energy are shown in **Table 2** [21, 44]. It is seen that the impact factor increases with decreasing X-ray energy. It is very large for Ni-$L\alpha_1$ (0.43 Å), Al $K\alpha_1$ (0.27 Å), Ta-$M\alpha_1$ and W-$M\alpha_1$ (0.23 Å), and decreases to 0.18 Å for Mo-$L\alpha_1$, and is in the range of 0.09 to 0.02 Å for X-ray energies larger than 4.5 keV (Ti-$K\alpha_1$, V-$K\alpha_1$, Cr-$K\alpha_1$, Co-$K\alpha_1$, Ni-$K\alpha_1$, Ta-$L\alpha_1$, W-$L\alpha_1$ and Mo-$K\alpha_1$). Thus, in order to reduce the delocalization effects, in the present calculation characteristic X-rays with an energy close to W-$L\alpha_1$ were evaluated using formula (3). Meanwhile, it is assumed that W is the hypo-stoichiometric element and fully occupies the *a* site, Co is the hyper-stoichiometric element and mainly occupies the other site in the $L1_2$ structure and Al also completely occupies the *a* site. By formula (3) the site occupancy of additional elements in the $L1_2$ structure have been calculated and the results are listed in **Table 3**. It is known that the accuracy of the site occupancy determination strongly depends on the channeling strength *E* [21, 45], which is defined as

$$E = \frac{|Y^k - Y^d|}{Y^k}, \tag{4}$$

where, Y_k and Y_d are the ratio N_W/N_{Co} under kinematical or dynamical conditions. The data points for the site occupancy (percentage of an alloying element on the W-site) obtained by formula (3) at each scattering condition were divided into three regimes $0<E<5$, $5<E<10$ and $E>10$ based on the channeling strength and their average values in each regime are shown in **Table 3**. When more measurement points were present in a range of channeling strength the standard deviation was calculated and this is also listed in **Table 3.** Most of the average site occupancy values in the weak channeling regime ($0<E<5$) show a huge scatter and are frequently unphysical being larger than unity or less than zero. For the higher channeling strengths, $5<E<10$ and $E>10$, the site occupancy values exhibit significantly reduced standard deviations of measurements. In addition, the diffraction vectors influence the channeling strength and thus affect the accuracy of the site occupancy determination. Using the scattering vectors vertical to the (022) Kikuchi band, the channeling strength is increased and more data points are located

in the strong channeling regime of E>10 compared to the measurements done with the scattering vectors perpendicular to the (002) Kikuchi band.

In the Co-9Al-9W alloy, the intensities of Al-K and W-M were inserted into the formula (3). It is found that in the strong channeling regime (E >10), the site occupancy of Al on the W site (94% or 108%) is close to unity, which supports our assumption for the quantitative analysis that Al fully occupies the W site in the $L1_2$ structure. For the alloying elements Ti, V, Cr and Ni in the Co-9Al-9W-2Ti, Co-9Al-9W-2V, Co-9Al-9W-2Cr, and Co-9Al-9W-2Ni alloys, respectively, the intensity of Ti-K, V-K, Cr-K, or Ni-K together with the W-L intensity have been used for the site occupancy calculations. The site occupancy for the elements Ti, V and Cr determined in the strong channeling regime (E >10) is always close to unity with values of (103±19) %, (94/106±15) % and (97±20) %, respectively. This also indicates that these elements exclusively occupy the W site in the $L1_2$ structure. However, for Ni the site occupancy ((18±47) % or (14±38) %) shows a huge scatter and is frequently close to zero for single measurements. This means that Ni does not favor the W site and tends to occupy the Co site. The intensity of Mo-K together with that of W-L or intensities of Mo-L and W-M have been used for the evaluation in the Co-9Al-9W-2Mo alloy and Ta/W-L or Ta/W-M used for the Co-9Al-9W-2Ta alloy. When using Mo-K/W-L and Ta/W-L X-ray energies for the calculations the results show a much stronger channeling strength and much smaller standard deviation of the data points than using Mo-L/W-M and Ta/W-M. (86/97±15) % Mo and (100±9/115±12) % Ta occupy the W site.

However, it has to be noted that the quantification results for Ni and Ta should be treated carefully due to the overlap of the corresponding characteristic X-ray peaks. To account for this during experiments the longest process time available with this analysis system was used to obtain spectra with the best peak resolution. This should help to reliably separate and resolve the overlapping peaks. Nevertheless, the data points of the normalized intensity and the site occupancy for Ni and Ta show obvious scatter. In the Co-9Al-9W-2Ta alloy, for quantifying the site occupancy the intensity of W-/Ta-M lines was used to reduce the delocalization effects as their energies were close to the energy of Al-K. This was also done by Horita et al. [43] for a $Ni_{75}Al_{21}Ta_4$ alloy. However, due to the overlap of the X-ray peaks, the deconvolution between W-/Ta-M seems to be not as easy as for W-/Ta-L. Thus for a better accuracy of the quantitative results, it is recommended to use the intensity of the W-/Ta-L lines for quantification. To

improve quantitative measurements of the site occupancy with the ALCHEMI technique in the $L1_2$ structure of Co-9Al-9W-2X alloys, the following potential ways are proposed. a. ALCHEMI investigations can be done at a lower temperature (e.g. liquid nitrogen temperature) to reduce the thermal displacement parameters and thus get a better channeling intensity; b. collecting more counts in a shorter time to get better statistic by tilting the specimen towards the detector (while maintaining defined diffraction conditions through choice of a suitably orientated part of the microstructure to analyze) or by using a four-quadrant FEI Super-X detector.

5.4 Comparison with literature data on site occupancy of alloying elements in the $L1_2$-γ' phase

It is very interesting to compare our results with the studies in literature. Based on the thermodynamic calculations of Ooshima et al. [4], V, Cr and Mo are predicted to preferentially partition into the disordered γ phase, Ni tends to occupy A-sites of the $L1_2$-A_3B phase and Ti and Ta favor the B-sites of the $L1_2$-A_3B phase. However, the results of first principle calculations performed by Chen et al. [10, 12] seem to partly contradict as it was found that Ni favored one of the three non-equivalent Co sites (in the supercell used for the calculation), Mo and Ta had a weak preference for the W site, while Cr, V, and Ti equally favored the face-centered Co site or the cube corner W site. There are also many experimental studies, in which a direct unambiguous experimental proof concerning the atomic site preference of alloying elements in the $L1_2$ structure is lacking and the site occupancy in the γ' phase has been determined by conclusions based on the chemical composition of the γ' phase [13-15, 46]. Povstugar et al. [13] found that in Co-9Al-9W, Co-9Al-9W-2Ti and Co-9Al-9W-2Ta alloys the Co fraction in the γ' phase was around 75-76 at.% and the remaining elements (Al, W, Ti or Ta) had a sum concentration of 24-25 at.%, which indicated that Al, W, Ti and Ta atoms occupied the B sublattice in the A_3B ($L1_2$-type) structure. In a Co-10Al-10W alloy investigated by Meher et al. [15] when Ta or Mo was added, the Co and Al contents remained unchanged while an equal fraction of W was replaced by Ta or Mo in the stoichiometric $L1_2$ γ' phase, which indicated that Ta and Mo occupied the W-sublattice in the $L1_2$ structure. In a Co-7Al-8W-4Ti-1Ta alloy studied by Chen et al. [17] using state of the art HRSTEM and super EDX techniques, Ti and Ta were confirmed to prefer the cube corner position in the same way as Al and W, while Co favored the face-center positions in the $L1_2$ structure. In a Cr containing Co(Ni)-Al-W superalloy investigated by Povstugar et al. [47] the phase composition measured by atom probe tomography indicated that Al, W and Cr tended to be

located at the B sublattice site in the γ'-A_3B phase, while Co and Ni occupied the A sublattice site. Thus, our results show good agreement with literature studies and can provide evidence to confirm the prediction on the site preference based on the phase composition in the literature.

As it has been explained in the introduction the site preference of alloying elements is a basic structural property which has significant influence on the constitution as well as the mechanical properties of the alloys. It is also needed for theoretical calculations of for example the thermodynamic stability [41] or the energy of planar faults. However, it is often difficult to separate the influence of the site occupancy on alloy properties from other alloying effects. It is found that the site occupancy of alloying elements does not unambiguously indicate their influences on the γ' solvus temperature and their partitioning behavior between the γ and γ' phases. With the addition of alloying elements such as Mo, V, Ti and Ta that preferentially partition into the γ' phase, the γ' solvus temperature increases when the alloying elements occupy the same sublattice site as Al and W [4-7, 48]. While the γ' solvus temperature does not change obviously when the alloying elements occupy the same site as Co in the γ' phase (Ni) or when they strongly partition into the γ matrix and occupy the same sublattice site as Al and W (Cr) [1, 5-7, 48]. Partitioning and site preference of alloying elements can also affect the lattice parameters of the γ and γ' phases and thus the lattice mismatch. Mo is reported to reduce the positive lattice misfit between γ and γ' phases in a multi-component Co-base superalloy [49]. Ta occupying the Al and W sublattice site is predicted by Density Functional Theory to increase the superlattice intrinsic stacking fault (SISF) energy of the γ' phase [50]. This can enhance the resistance of the γ' phase to initial shearing by a/3<112> dislocations, resulting in strengthening effects in the Ta containing Co-base superalloys [50].

6. Conclusions

In this study, the atomic site occupancy of alloying elements in the $L1_2$-γ' structure in the Co-9Al-9W-2X quaternary alloys was investigated in detail by the experimental and quantitative ALCHEMI analysis together with inelastic scattering cross-section calculations and EDX phase composition analysis after annealing at 900 °C for 5000 h. It is found that Co atoms mainly occupy one sublattice site and Al/W take the other sublattice site in the $L1_2$ unit cell as previously indicated in the literature. The additional elements Ti, V, Cr, Mo and Ta tend to occupy the sublattice site of the Al/W atoms, while Ni favors the Co sublattice site. To the authors' knowledge, this is the first ALCHEMI study in γ-γ' Co-base superalloys

which can provide evidence for the predictions on the site preference in literature that were based on the phase composition or from theoretical studies. The main conclusions of the study are:

1) Experimental parameters such as electron voltage, specimen thickness and convergence angle can affect the enhancement of the characteristic X-rays and thus the channeling intensity in the experimental ALCHEMI investigation. A voltage of 200 kV and a convergence angle of 4 mrad (the largest condenser aperture) with a specimen thickness in the range of 100 to 200 nm were used and worked well for determining the site preference of alloying elements in the $L1_2$ structure of Co-9Al-9W-2X quaternary alloys.
2) The site preference of alloying elements can be determined by experimental ALCHEMI and the experimental ALCHEMI results were evaluated by comparing them with calculations of the inelastic cross section done by using the program ICSC (Inelastic Cross Section Calculator) developed by Oxley and Allen [32].
3) In the ternary alloy, the phase composition of the γ' phase does slightly deviate from the stoichiometric ratio and has an excess in Co and a deficiency in Al. Additional elements in the quaternary system can be classified into three groups. a. Mo, V, Ti and Ta preferentially partition into the γ' phase and occupy the Al/W site; b. Cr partitions to the γ phase but occupies the Al/W site when present in the γ' phase; c. Ni weakly partitions into the γ' phase and occupies the Co site.
4) The formula developed by Horita et al. [43] can be used for quantitative ALCHEMI analysis. By using this formula the influence from X-ray energy absorption can be excluded. The delocalization effects can be greatly reduced by using characteristic X-ray radiation of similar energy for calculation.
5) For scattering vectors perpendicular to the (110) Kikuchi band a better channeling strength and more reliable quantitative results for the site occupancy were obtained than using scattering vectors vertical to the (001) Kikuchi band.
6) Around 100 % of the elements Ti, V, Cr, Mo and Ta in the alloys occupy the Al/W site in the $L1_2$ structure. While for Ni, the site occupancy on the Al/W site has been determined to be (18±47) %

and (14±38) % when using scattering vectors perpendicular to the (001) and (011) Kikuchi bands, respectively. This strongly suggests that Ni occupies the Co site in the $L1_2$ structure.

Acknowledgements

Li Wang acknowledges the Helmholtz Association for funding her Postdoc project at Helmholtz-Zentrum Geesthacht in the framework of the Helmholtz Postdoc Program. The authors are very grateful to Dr. Jonathan Paul for the revision of the English.

References

[1] J. Sato, T. Omori, K. Oikawa, I. Ohnuma, R. Kainuma, K. Ishida, Cobalt-base high-temperature alloys, Science 312 (2006) 90-91.
[2] T.M. Pollock, J. Dibbern, M. Tsunekane, J. Zhu, A. Suzuki, New Co-based γ-γ′ high-temperature alloys, JOM 62 (2010) 58-63.
[3] E.A. Lass, M.E. Williams, C.E. Campbell, K.W. Moon, U.R. Kattner, γ′ phase stability and phase equilibrium in ternary Co-Al-W at 900 °C, Phs. Eqil. Diff. 35 (2014) 711-723.
[4] M. Ooshima, K. Tanaka, N.L. Okamoto, K. Kishida, H. Inui, Effects of quaternary alloying elements on the γ′ solvus temperature of Co–Al–W based alloys with fcc/$L1_2$ two-phase microstructures, J. Alloy. Compd. 508 (2010) 71-78.
[5] A. Suzuki, H. Inui, T.M. Pollock, $L1_2$-strengthened cobalt-base superalloys, Ann. Rev. Mater. Res. 45 (2015) 345-368.
[6] A. Bauer, S. Neumeier, F. Pyczak, M. Göken, Microstructure and creep strength of different γ/γ′-strengthened Co-base superalloy variants, Scripta Mater. 63 (2010) 1197-1200.
[7] T. Omori, K. Oikawa, J. Sato, I. Ohnuma, U.R. Kattner, R. Kainuma, K. Ishida, Partition behavior of alloying elements and phase transformation temperatures in Co–Al–W-base quaternary systems, Intermetallics 32 (2013) 274-283.
[8] A. Bauer, S. Neumeier, F. Pyczak, M. Göken, Creep strength and microstructure of polycrystalline γ′- strengthened cobalt-base superalloys, in: E.S. Huron, M.C. Hardy, M.J. Mills, R.E. Montero, P.D. Portella, J. Telesman (Ed.), 12th International Symposium on Superalloys, TMS (The Minerals, Metals & Materials Society), 2012, pp. 695-703.
[9] K. Shinagawa, T. Omori, J. Sato, K. Oikawa, I. Ohnuma, R. Kainuma, K. Ishida, Phase equilibria and microstructure on γ′ phase in Co-Ni-Al-W system, Mater. Trans. 49 (2008) 1474-1479.
[10] M. Chen, C.Y. Wang, First-principles investigation of the site preference and alloying effect of Mo, Ta and platinum group metals in γ′-Co_3(Al, W), Scripta Mater. 60 (2009) 659-662.
[11] J. Koßmann, T. Hammerschmidt, S. Maisel, S. Müller, R. Drautz, Solubility and ordering of Ti, Ta, Mo and W on the Al sublattice in $L1_2$-Co_3Al, Intermetallics 64 (2015) 44-50.
[12] M. Chen, C.Y. Wang, First-principle investigation of transition metal elements in γ′-Co_3(Al, W), J. Appl. Phys. 107 (2010) 093705.
[13] I. Povstugar, P.P. Choi, S. Neumeier, A. Bauer, C.H. Zenk, M. Göken, D. Raabe. Elemental partitioning and mechanical properties of Ti- and Ta-containing Co–Al–W-base superalloys studied by atom probe tomography and nanoindentation, Acta Mater. 78 (2014) 78-85.
[14] S. Meher, H.Y Yan, S. Nag, D. Dye, R. Banerjee, Solute partitioning and site preference in γ/γ′ cobalt-base alloys, Scripta Mater. 67 (2012) 850-853.
[15] S. Meher, R. Banerjee, Partitioning and site occupancy of Ta and Mo in Co-base γ/γ′ alloys studied by atom probe tomography, Intermetallics 49 (2014) 138-142.
[16] H.J. Im, S.K. Makineni, B. Gault, F. Stein, D. Raabe, P.-P. Choi, Elemental partitioning and site-occupancy in γ/γ′ forming Co-Ti-Mo and Co-Ti-Cr alloys, Scripta Mater. 154 (2018) 159-162.
[17] Y. Chen, F. Xue, S. Mao, H. Long, B. Zhang, Q. Deng, B. Chen, Y. Liu, P. Maguire, H. Zhang, X. Han, Q. Feng, Elemental preference and atomic scale site recognition in a Co-Al-W-base superalloy, Scientific Reports 7 (2017) 17240.

[18] J.C.H. Spence, J. Taftø, ALCHEMI: a new technique for locating atoms in small crystals, Journal of Microscopy 130 (1983)147-154.
[19] J. Taftø, J.C.H. Spence, Crystal Site Location of Iron and Trace Elements in a Magnesium-Iron Olivine by a New Crystallographic Technique, Science 218 (1982) 49-51.
[20] S.C. Huang, E.L. Hall, Characterization of the effect of vanadium additions to TiAl base alloys, Acta Metall. Mater. 39 (1991) 1053-1060.
[21] C.H. Liebscher, J. Preussner, R. Voelkl, U. Glatzel, Atomic site location by channelling enhanced microanalysis (ALCHEMI) in γ′-strengthened Ni- and Pt-base alloys, Acta Mater. 56 (2008) 4267-4276.
[22] L.M. Pike, I.M. Anderson, C.T. Liu, Y.A. Chang, Site occupancies, point defect concentrations, and solid solution hardening in B2 (Ni,Fe)Al, Acta Mater. 50 (2002) 3859-3879.
[23] H. Okaniwa, D. Shindo, M. Yoshida, T. Takasugi, Determination of site occupancy of additives X (X=V, Mo, W and Ti) in the Nb–Cr–X Laves phase by ALCHEMI, Acta Mater. 47 (1999) 1987-1992.
[24] P.R. Munroe, I. Baker, Effect of accelerating voltage on planar and axial channeling in ordered intermetallic compounds, J. Mater. Res. 7 (1992) 2119-2125.
[25] M.P. Oxley, L.J. Allen, C.J. Rossouw, Correction terms and approximations for atom location by channelling enhanced microanalysis, Ultramicroscopy 80 (1999)109-124.
[26] S.J. Pennycook, Delocalization corrections for electron channeling analysis, Ultramicroscopy 26 (1988) 239-248.
[27] I.M. Anderson, ALCHEMI study of site distributions of 3d-transition metals in B2-ordered iron aluminides, Acta Mater. 45 (1997) 3897-3909.
[28] Z. Horita, General formulation for ALCHEMI including delocalization effect, Ultramicroscopy 66 (1996) 1-4.
[29] C.J. Rossouw, P.S. Turner, T.J. White A. O'Connor, Statistical analysis of electron channelling microanalytical data for the determination of site occupancies of impurities, J. Philos. Mag. Lett. 60 (1989) 225.
[30] P.S. Turner, T.J. White, A.J . O'Connor, C.J. Rossouw, Advances in ALCHEMI analysis, Journal of Microscopy 162 (1991) 369-378.
[31] M.G. Walls, Multivariate alchemi in the presence of anti-site defects, Journal De Physique, 3 (1993) 2155-2158.
[32] M.P. Oxley, L.J. Allen, *ICSC*: a program for calculating inelastic scattering cross sections for fast electrons incident on crystals, J. Appl. Crystallogr. 36 (2003) 940-943.
[33] T. Morimura, M. Hasaka, ALCHEMI for coexistent Heusler and half-Heusler phases in $TiNi_{1.5}Sn$, Ultramicroscopy 106 (2006) 553-560.
[34] M. Meffert, H. Störmer, D. Gerthsen, Dopant-site determination in Y- and Sc-doped $(Ba_{0.5}Sr_{0.5})(Co_{0.8}Fe_{0.2})O_{3-\delta}$ by atom location by channeling enhanced microanalysis and the role of dopant site on secondary phase formation, Microsc. Microanal. 22 (2016) 113-121.
[35] L.J. Allen, T.W. Josefsson, C.J. Rossouw, Interaction delocalization in characteristic X-ray emission from light elements, Ultramicroscopy 55 (1994) 258-267.
[36] L.M. Peng, G. Ren, S.L. Dudarev, M.J. Whelan, Debye-Waller factors and absorptive scattering factors of elemental crystals, Acta Crystallogr. A 52 (1996) 456-470.
[37] Y. Nakata, T. Tadaki, K. Shimizu, Evaluation of accuracy in the ALCHEMI method, Ultramicroscopy 39(1991) 72-80.
[38] K.M. Krishnan, Atomic site and species determinations using channeling and related effects in analytical electron microscopy, Ultramicroscopy 24 (1988) 125-141.
[39] C.J. Rossouw, C.T. Forwood, M.A. Gibson, P.R. Miller, Generation and absorption of characteristic X-rays under dynamical electron diffraction conditions, Micron 28 (1997) 125-137.
[40] L. Wang, M. Oehring, U. Lorenz, J.J. Yang, F. Pyczak, Influence of alloying additions on $L1_2$ decomposition in γ-γ′ Co-9Al-9W-2X quaternary alloys, Scripta Mater. 154 (2018) 176-181.
[41] P.J. Bocchini, E.A. Lass, K.W. Moon, M.E. Williams, C.E. Campbell, U.R. Kattner, D.C. Dunand, D.N. Seidman, Atom-probe tomographic study of γ/γ′ interfaces and compositions in an aged Co–Al–W superalloy, Scripta Mater. 68 (2013) 563-566.
[42] J. E. Saal, C. Wolverton, Thermodynamic stability of Co–Al–W $L1_2$ γ′, Acta Mater. 61 (2013) 2330-2338.
[43] Z. Horita, S. Matsumura, T. Baba, General formulation for ALCHEMI, Ultramicroscopy 58 (1995)

327-335.
[44] M.P. Oxley, L.J. Allen, Impact parameters for ionization by high-energy electrons, Ultramicroscopy 80 (1999) 125-131.
[45] C.J. Rossouw, C.T. Forwood, M.A. Gibson, P.R. Miller, Statistical ALCHEMI: general formulation and method with application to Ti-Al ternary alloys, Philos. Mag. A 74 (1996) 57-76.
[46] P.J. Bocchini, C.K. Sudbrack, R.D. Noebe, D.C. Dunand, D.N. Seidman, Effect of titanium substitutions for aluminum and tungsten in Co-10Ni-9Al-9W (at%) superalloys, Mater. Sci. Eng. A 705 (2017) 122-132.
[47] I. Povstugar, C.H. Zenk, R. Li, P.P. Choi, S. Neumeier, O. Dolotko, M. Hoelzel, M. Göken, D. Raabe, Elemental partitioning, lattice misfit and creep behaviour of Cr containing gamma' strengthened Co base superalloys, Mater. Sci. Technol. 32 (2016) 220-225.
[48] L. Wang, Microstructure, phase stability and element partitioning in the γ-γ’ Co-9Al-9W-2X alloys at different annealing conditions, unpublished results, 2018.
[49] M.S. Titus, A. Suzuki, T.M. Pollock, Creep and directional coarsening in single crystals of new γ–γ′ cobalt-base alloys, Scripta Mater. 66 (2012) 574-577.
[50] A. Mottura, A. Janotti, T.M. Pollock, A first-principles study of the effect of Ta on the superlattice intrinsic stacking fault energy of $L1_2$-Co3(Al,W), Intermetallics 28 (2012) 138-143.

Table 1 Chemical compositions of the γ' phase in Co-9Al-9W-2X alloys by TEM-EDX analysis.

Alloy (at.%)	Co	Al	W	X	$K_{\gamma'/\gamma}$
Co-9Al-9W	78.8±0.4	9.2±0.2	12.1±0.3	/	/
Co-9Al-9W-2Ti[40]	78.7±0.4	8.3±0.3	10.5±0.3	2.5±0.1	2.2
Co-9Al-9W-2V	78.9±0.2	8.5±0.2	10.3±0.1	2.3±0.1	1.3
Co-9Al-9W-2Mo[40]	78.3±0.3	9.0±0.2	10.4±0.2	2.4±0.1	1.2
Co-9Al-9W-2Ta[40]	78.3±0.2	8.8±0.1	10.2±0.2	2.7±0.1	6.3
Co-9Al-9W-2Cr	78.1±0.3	8.8±0.1	11.3±0.3	1.8±0.1	0.6
Co-9Al-9W-2Ni	77.4±0.2	8.8±0.3	11.9±0.2	1.9±0.1	1.1

Table 2 Root-mean square impact parameter b_{rms} of the characteristic X-rays of alloying elements with 200 keV electrons [21, 44].

X-ray energy (keV)	b_{rms} (Å)
Ni-$L\alpha_1$ (0.85)	0.43
Al-$K\alpha_1$ (1.49)	0.27
Ta-$M\alpha_1$ (1.71)	0.23
W-$M\alpha_1$ (1.78)	0.23
Mo-$L\alpha_1$ (2.29)	0.18
Ti-$K\alpha_1$ (4.51)	0.09
V-$K\alpha_1$ (4.95)	0.08
Cr-$K\alpha_1$ (5.41)	0.07
Co-$K\alpha_1$ (6.93)	0.06
Ni-$K\alpha_1$ (7.48)	0.05
Ta-$L\alpha_1$ (8.15)	0.05
W-$L\alpha_1$ (8.40)	0.04
Mo-$K\alpha_1$ (17.48)	0.02

Table 3 Percentage (site occupancy) of alloying elements on the W-site in the $L1_2$ structure by quantitative ALCHEMI analysis (*E*: channeling strength).

Alloy (at.%)	Characteristic X-ray	Scattering Vector	Site occupancy on W-site (%)		
			0<*E*<5	5<*E*<10	*E>10*
Co-9Al-9W	Al-K (W-M)	g_{100}	62±150	88±18	94
		$g_{1\text{-}10}$	351±302	114±15	108±1
Co-9Al-9W-2Ti	Ti-K (W-L)	g_{001}	49±226	98±25	/
		g_{011}	50±148	75±27	103±19
Co-9Al-9W-2V	V-K (W-L)	g_{001}	73±57	102±25	94±15
		g_{011}	84±35	95±16	106±15
Co-9Al-9W-2Mo	Mo-K (W-L)	$g_{1\text{-}10}$	210±93	104±30	97±15
	Mo-L (W-M)		119±140	67±57	86
Co-9Al-9W-2Ta	Ta-L (W-L)	g_{001}	127±41	135±37	115±12
	Ta-M (W-M)		1955±5799	136±75	100±9
Co-9Al-9W-2Cr	Cr-K (W-L)	g_{011}	146±429	118±20	97±20
Co-9Al-9W-2Ni	Ni-K (W-L)	g_{001}	108±540	48±51	18±47
		g_{011}	-2823±8444	-13±23	14±38

The numbers after "±" are standard deviation of measurements.

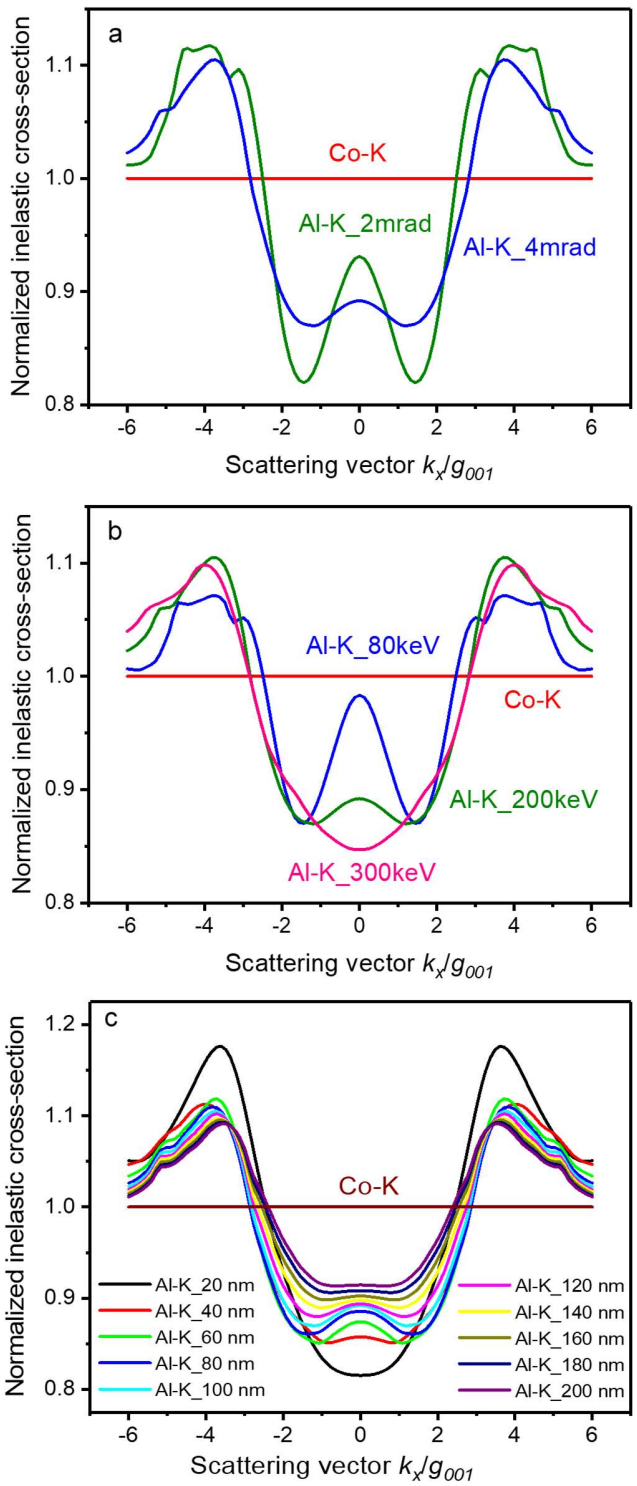

Figure 1 Influence of parameters on the profiles of calculated normalized inelastic cross-sections plotted against k_x/g_{001} near the [100] direction. (a) Convergence angle, (b) voltage, and (c) specimen thickness. The cross-sections were firstly normalized by the cross-sections under kinematical condition and then normalized by the cross-sections of the Co-K.

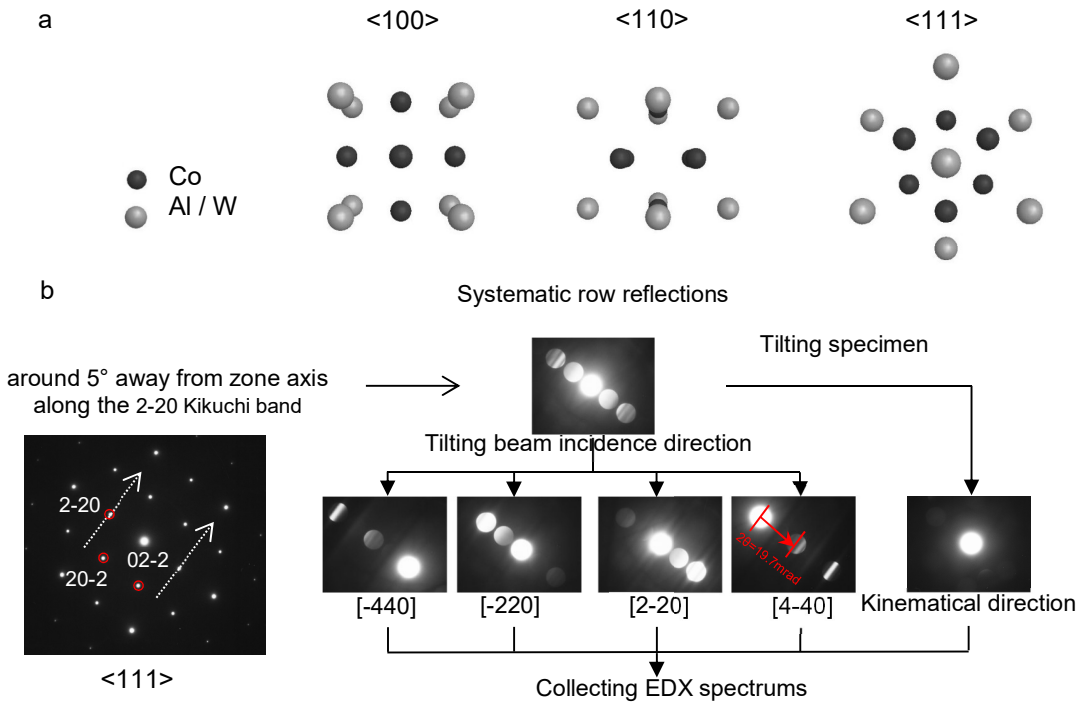

Figure 2 (a) Channeling zone axis orientations of the $L1_2$-structure $Co_3(Al, W)$ phase, (b) schematic illustration of planar ALCHEMI experiment near to the <111> zone axis orientation of the $Co_3(Al, W)$ phase.

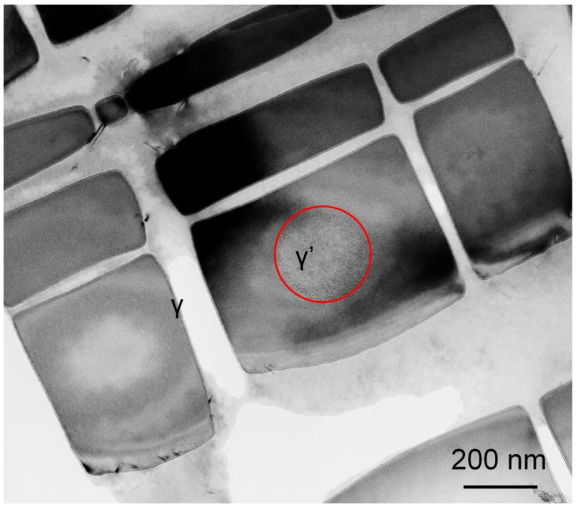

Figure 3 TEM image of the Co-9Al-9W alloy after annealing at 900 °C for 5000 h. The EDS measurement was done in the γ' region marked by a circle. Contamination can be observed after the experiment.

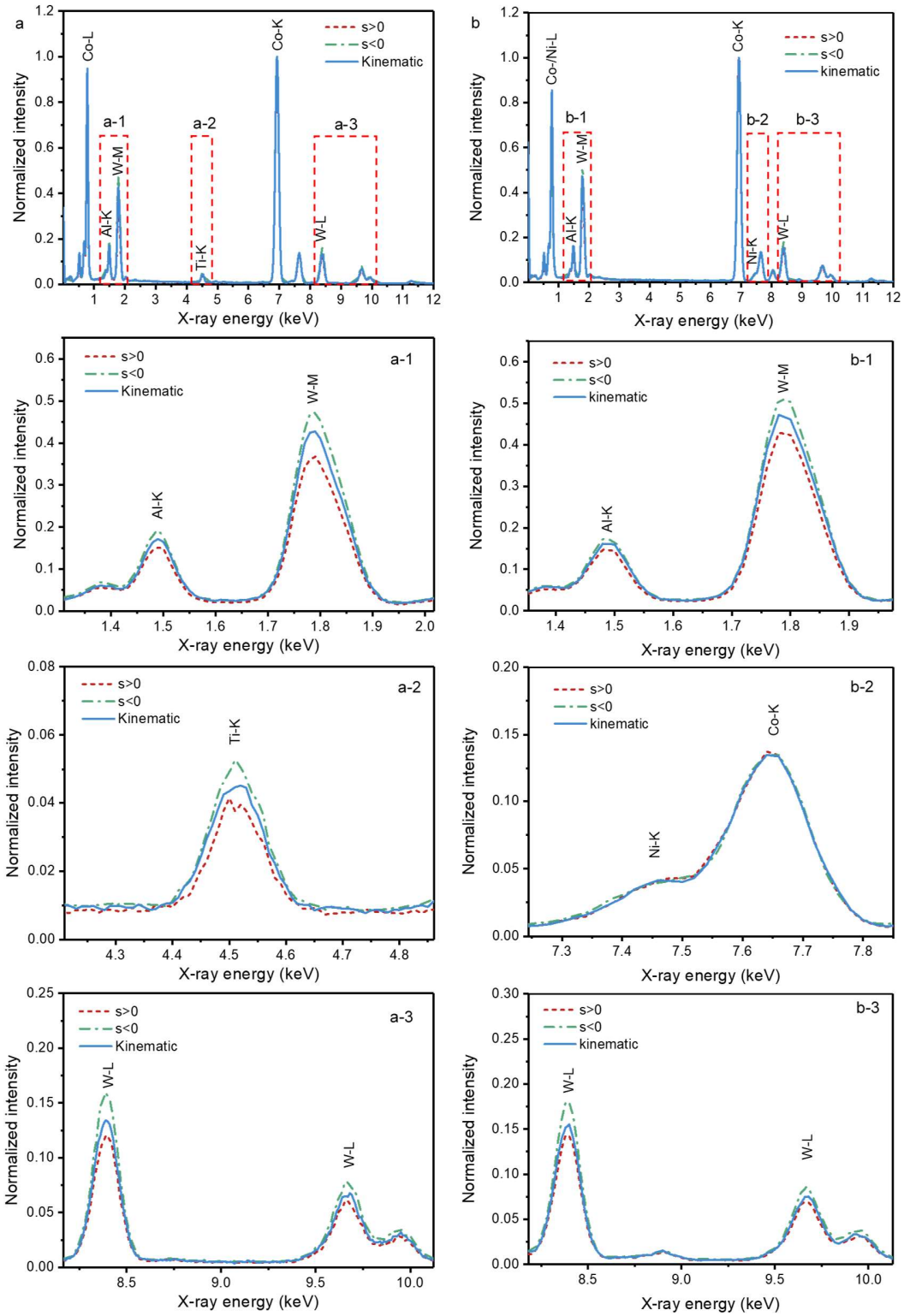

Figure 4 EDX spectra of the (a) Co-9Al-9W-2Ti and (b) Co-9Al-9W-2Ni alloys collected near the <100> orientation along the 022 Kikuchi band at *s*>0, *s*<0 with respect to the 011 reflection and kinematical scattering conditions. The intensity was normalized to that of the Co-K peak.

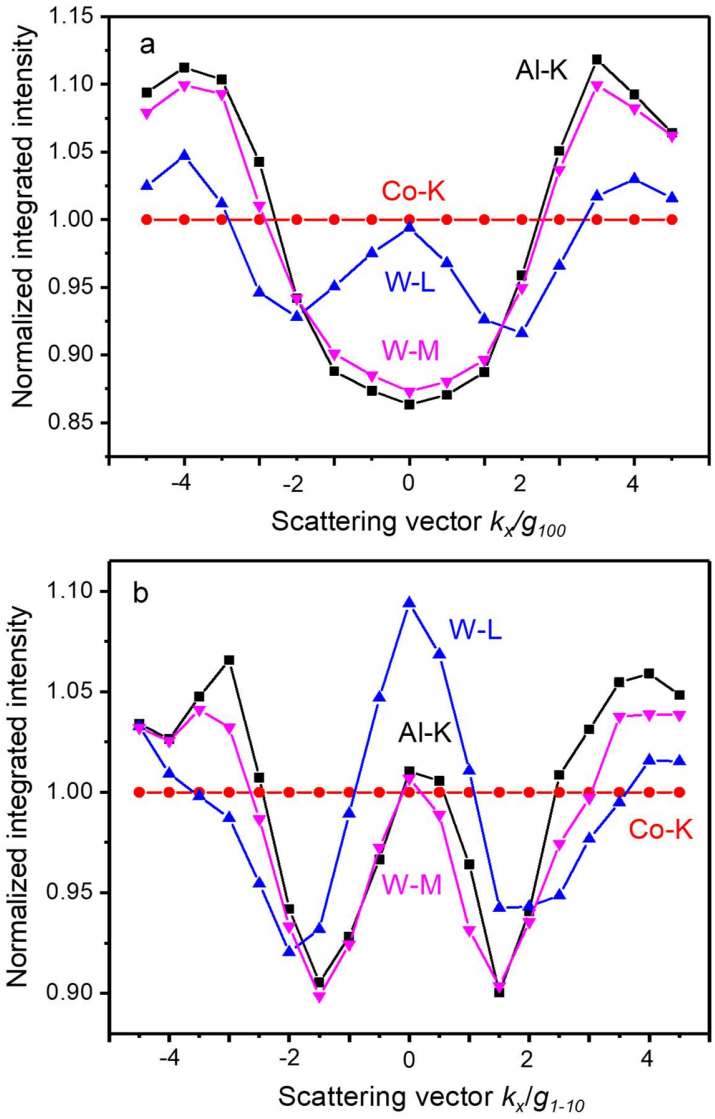

Figure 5 Measured normalized X-ray intensity profiles in the Co-9Al-9W alloy plotted against (a) k_x/g_{100} near the <011> direction and (b) $k_x/g_{1\text{-}10}$ near the <111> direction. The intensities were first normalized by the intensities under kinematical condition and then normalized by the intensities of the Co-K.

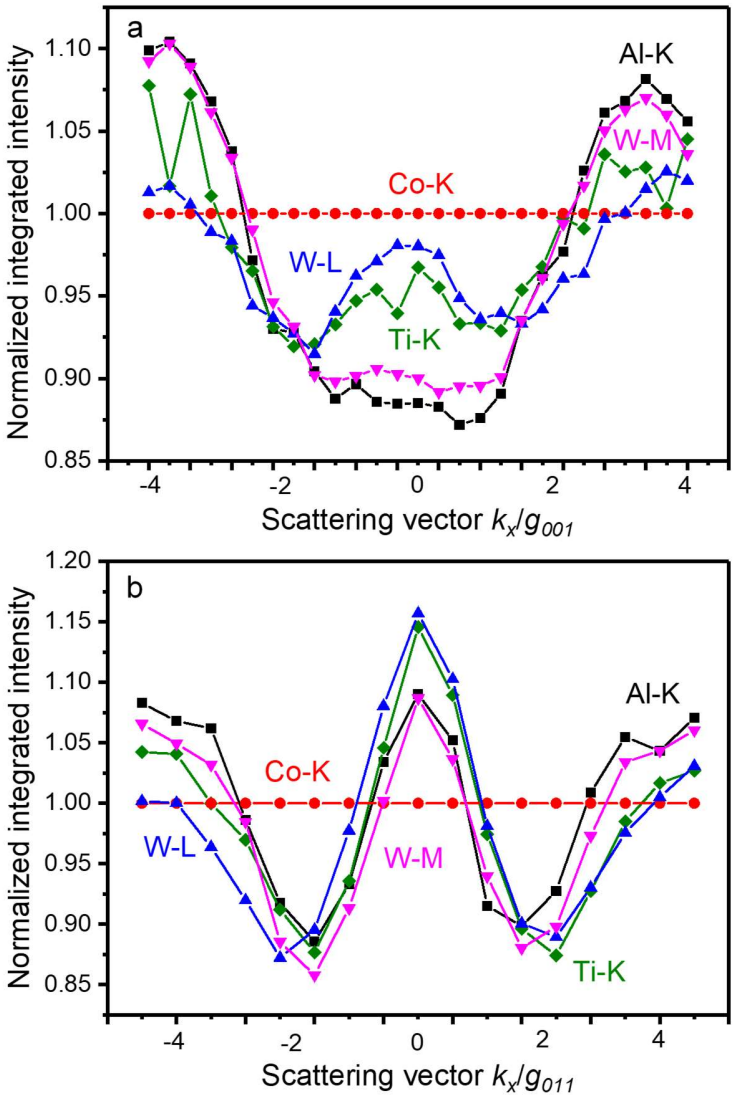

Figure 6 Measured normalized X-ray intensity profiles in the Co-9Al-9W-2Ti alloy plotted against (a) k_x/g_{001} and (b) k_x/g_{011} near the <100> direction. The intensities were firstly normalized by the intensities under kinematical condition and then normalized by the intensities of the Co-K.

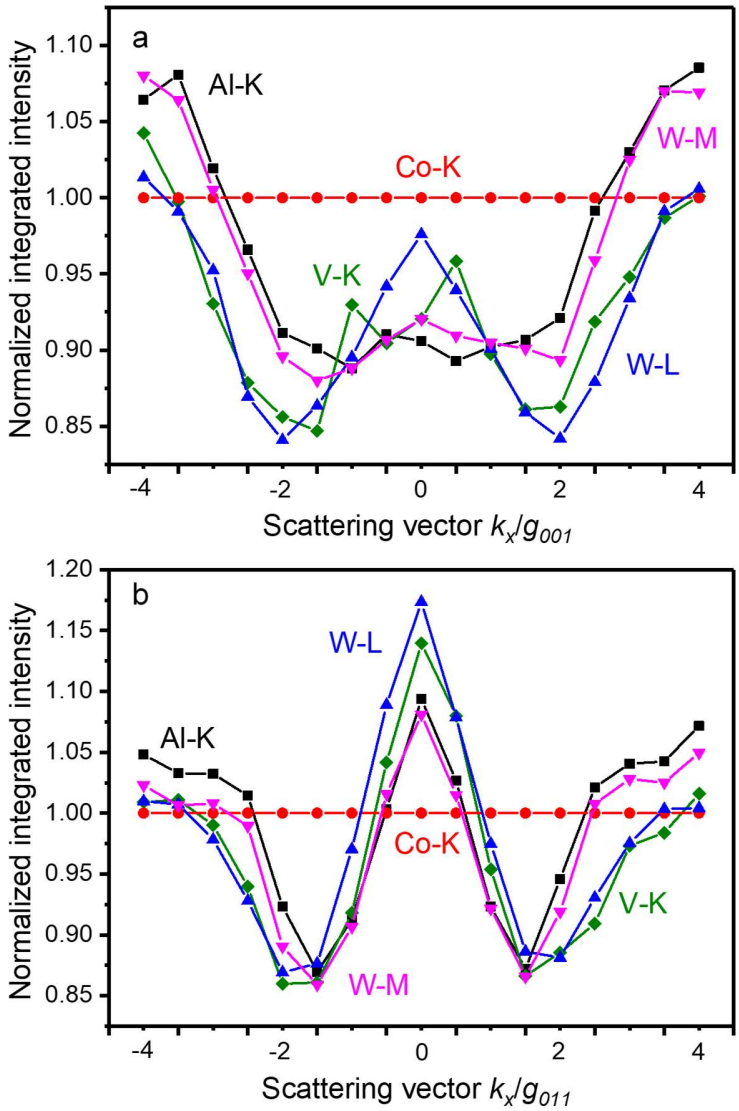

Figure 7 Measured normalized X-ray intensity profiles in the Co-9Al-9W-2V alloy plotted against (a) k_x/g_{001} and (b) k_x/g_{011} near the <100> direction. The intensities were firstly normalized by the intensities under kinematical condition and then normalized by the intensities of the Co-K.

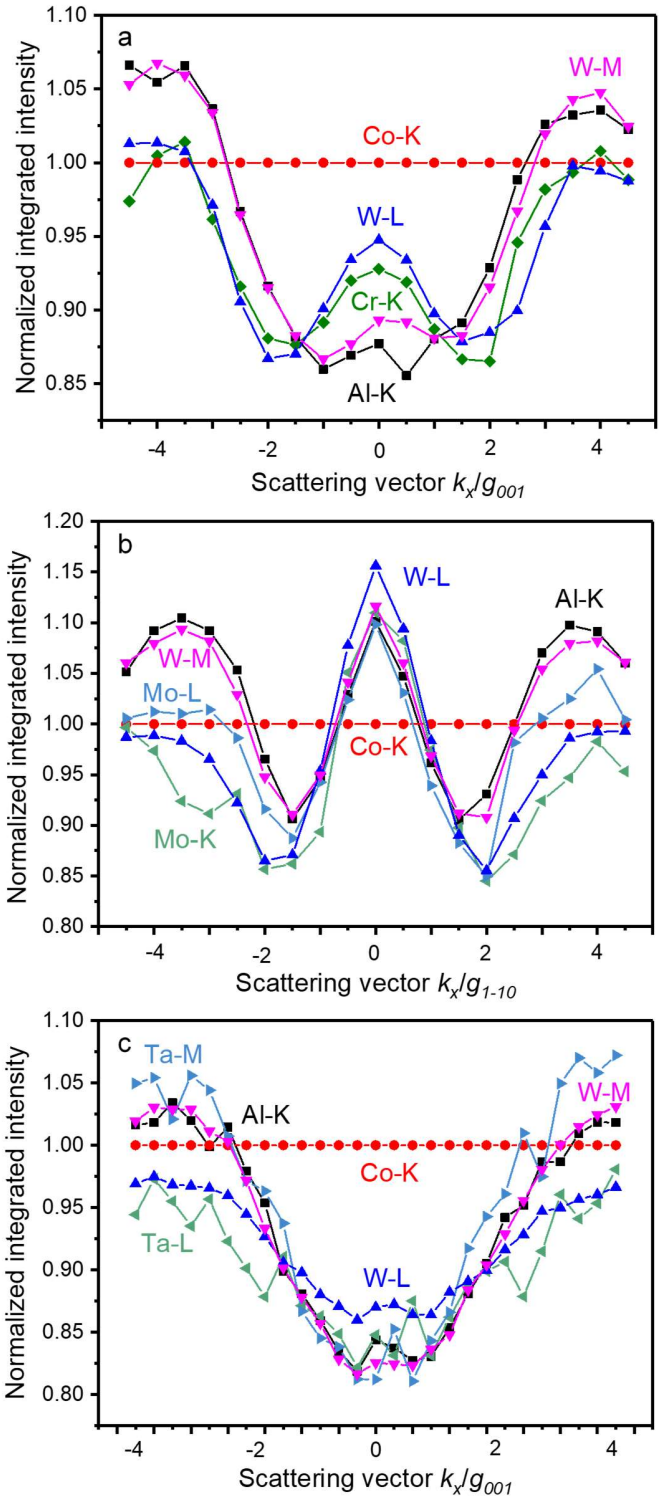

Figure 8 Measured normalized X-ray intensity profiles plotted against (a) k_x/g_{001} near the <100> direction in the Co-9Al-9W-2Cr alloy, (b) $k_x/g_{1\text{-}10}$ near the <110> direction in the Co-9Al-9W-2Mo alloy and (c) k_x/g_{001} near the <100> direction in the Co-9Al-9W-2Ta alloy. The intensities were firstly normalized by the intensities under kinematical condition and then normalized by the intensities of the Co-K.

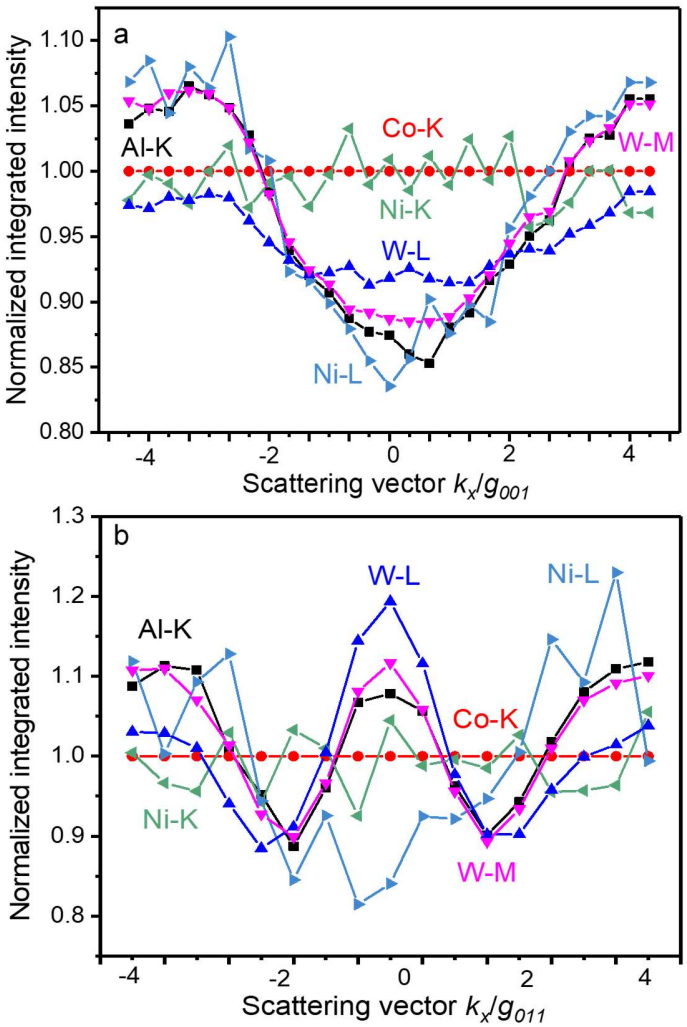

Figure 9 Measured normalized X-ray intensity profiles in the Co-9Al-9W-2Ni alloy plotted against (a) k_x/g_{001} and (b) k_x/g_{011} near the <100> direction. The intensities were firstly normalized by the intensities under kinematical condition and then normalized by the intensities of the Co-K.

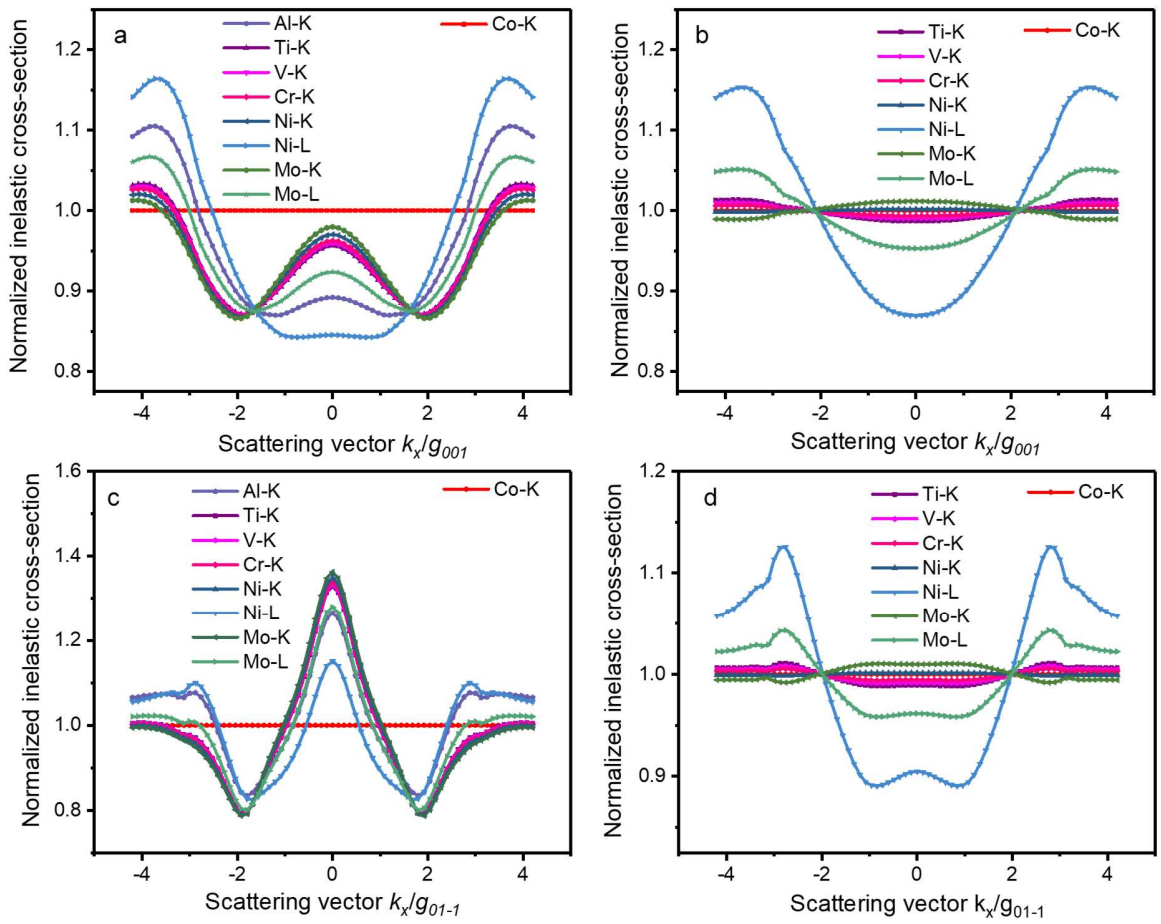

Figure 10 Calculated normalized inelastic cross-sections plotted against (a, b) k_x/g_{001} and (c, d) k_x/g_{01-1} near the <100> orientation. In (a, c), alloying elements occupy the Al-site and (b, d) alloying elements occupy the Co-site. The cross-sections were first normalized by those under kinematical condition and then by the cross-section of the Co-K.